17th ASCE Engineering Mechanics Conference
June 13–16, 2004, University of Delaware, Newark, DE

EM2004

ISOLATION OF NON-HYDROSTATIC REGIONS WITHIN A BASIN

Bridget M. Wadzuk[1] (Member, ASCE) and Ben R. Hodges[2] (Member, ASCE)

ABSTRACT

Modeling of dynamic pressure appears necessary to achieve a more robust simulation of the events within a stratified basin; however, its effects are typically spatially and temporally limited. The overall computational expense associated with the dynamic pressure can be reduced if the non-hydrostatic regions can be identified prior to the dynamic pressure calculation. In this work, we seek to define an appropriate criterion that can be computed from a hydrostatic solution and used as an indicator of the possible magnitude of non-hydrostatic effects.

Keywords: dynamic pressure, internal wave, hydrodynamic model

INTRODUCTION

The inclusion of dynamic pressure in hydrodynamic models can increase a model's skill in capturing the small-scale phenomena of internal wave evolution. However, the dynamic pressure solution can significantly increase computational expense (approximately two orders of magnitude longer than the computational time for a similarly-scaled hydrostatic model), thus making the inclusion of non-hydrostatic effects impractical for many systems. Most basins of interest (lakes, estuaries and coastal oceans) typically conform to the hydrostatic condition and deviate only in select regions of the basin and for limited periods of time. It would be advantageous if a non-hydrostatic model is applied only in regions that deviated from the hydrostatic condition, while a more economical hydrostatic model is applied to the remaining portion of the domain. This could reduce computational expense and increase the model's skill in capturing internal wave evolution. Stansby and Zhou (1998) proposed this idea, however they did not implement or test any algorithm for spatially or temporally isolated pressure solutions. The present work investigates the practicality of isolating the dynamic pressure calculation to non-hydrostatic regions of a computational domain.

DISCUSSION

The governing equations used are the incompressible, Reynolds-averaged Navier Stokes equations with the Bousinessq approximation and a free-surface solution. The model used in this

[1] Corresponding author: Department of Civil Engineering, The University of Texas at Austin, Austin, TX 78712, USA, email: bwadzuk@mail.utexas.edu, fax: 512-471-0072

[2] Department of Civil Engineering, The University of Texas at Austin, Austin, TX 78712, USA

study is the Centre for Water Research Estuary and Lake Computer Model, CWR-ELCOM (Hodges, 2000a). This model is a three-dimensional hydrodynamic model that simulates fluid flows for stratified bodies with the hydrostatic approximation. CWR-ELCOM was modified by the authors to include a dynamic pressure solver. The fractional step method (Kim and Moin, 1985) was used to incorporate the dynamic pressure solver into the existing model. The first step applies the hydrostatic CWR-ELCOM to resolve the hydrostatic velocity field. The resulting hydrostatic velocity field is used to solve a pressure Poisson equation in the second step; subsequently the pressure, velocity, and free-surface fields are updated. It is between the two steps of the fractional step method that the non-hydrostatic regions can be identified and isolated, thus not requiring the pressure Poisson solution over the entire domain.

For a system to meet the hydrostatic condition, the dynamic pressure term must be significantly smaller than the other terms (specifically, acceleration) in the horizontal equations of motion (Hodges, 2000b). The system is considered non-hydrostatic when the dynamic pressure term is of equal or greater magnitude than the other terms in these equations. Assuming the local horizontal acceleration term is the leading term in the horizontal momentum equation, a "non-hydrostatic factor" is proposed as:

$$\gamma \equiv \frac{\left(-\frac{1}{\rho}\frac{\partial p_d}{\partial x} \right)}{\left(\frac{\partial u}{\partial t} \right)} \tag{1}$$

The hydrostatic velocity is used in the denominator, while it is desirous to approximate the expected dynamic pressure gradient so that the non-hydrostatic factor can be estimated prior to the Poisson solution. The non-hydrostatic factor captures the physical behavior of the basin, as well as the spatial discretization. It is necessary to capture both of these aspects because an internal wave may behave non-hydrostatically (i.e. steepening wave front), however the grid scale chosen may dwarf the effect of the non-hydrostatic behavior. In example, a wave may be nonlinearly steepening and dynamic pressure present, however if the grid scale is such that the horizontal grid length is much larger than the vertical grid length, than the steepened wave front may not be properly captured.

To approximate the dynamic pressure gradient, we note that the vertical momentum equation for inviscid flow is:

$$\frac{Dw}{Dt} = -\frac{1}{\rho}\frac{\partial p_d}{\partial z} \tag{2}$$

The hydrostatic approximation neglects vertical acceleration and dynamic pressure in the Navier-Stokes equations, essentially eliminating the vertical momentum equation. The hydrostatic vertical velocity is determined by diagnostically satisfying continuity based on the hydrostatic horizontal velocity, so the vertical velocity reflects divergence in the horizontal flow field. Two approaches were examined to model the vertical dynamic pressure gradient: the total acceleration term, as in eq. (2), and the nonlinear acceleration term. When the hydrostatic velocities are used in eq. (2), the local vertical acceleration, $\partial w / \partial t$, dominates the total acceleration term and clearly shows the accumulation of error in the calculation of vertical velocity from continuity. The local

acceleration term does not compare well to the vertical pressure gradient resulting from the non-hydrostatic model. The second approach used the nonlinear component as the model to the vertical dynamic pressure gradient:

$$u\frac{\partial w}{dx}+w\frac{\partial w}{dz}=-\frac{1}{\rho}\frac{\partial p_d}{\partial z} \tag{3}$$

When the hydrostatic velocities are applied to eq. (3), the nonlinear term did compare well with the vertical dynamic pressure gradient from the non-hydrostatic model. Fig. (1) shows the comparison of the vertical dynamic pressure gradient from the non-hydrostatic model and the hydrostatic model vertical dynamic pressure gradient when the nonlinear approach is used.

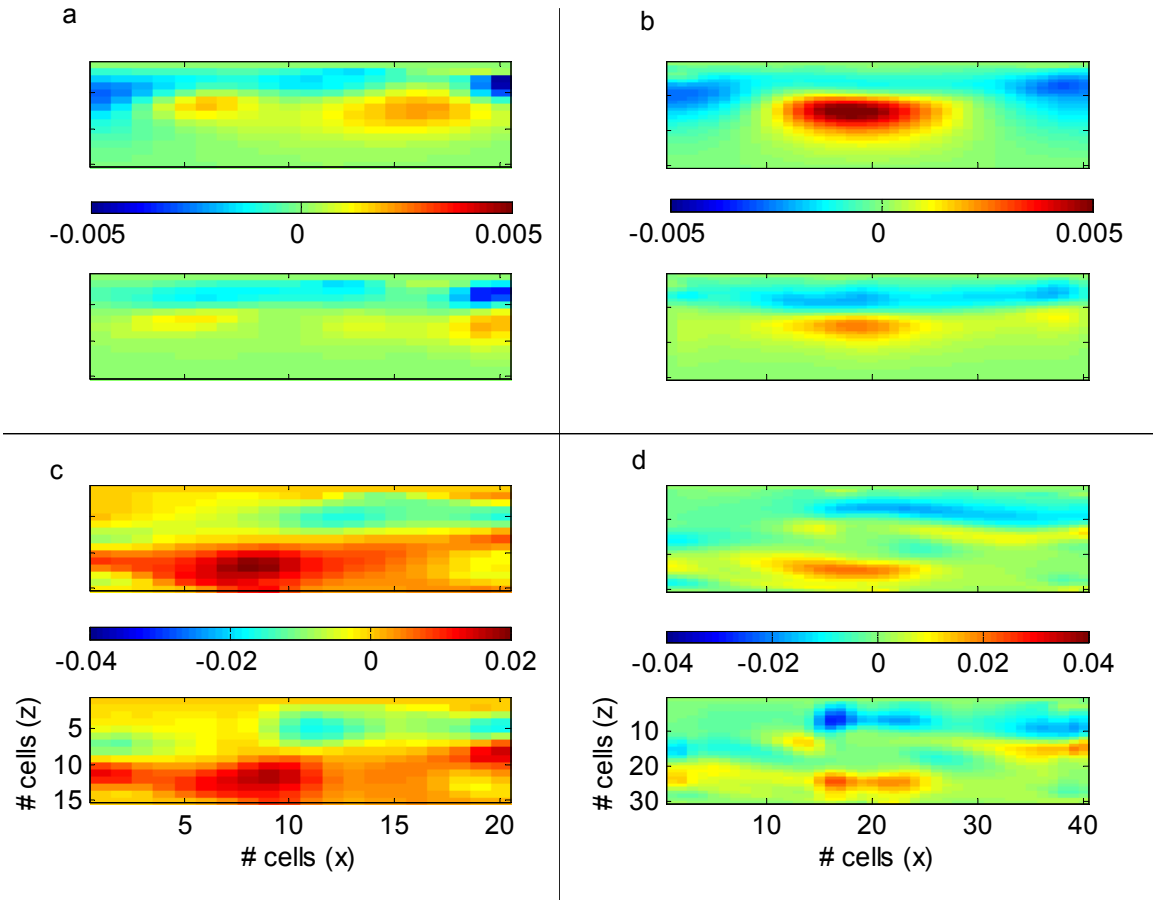

FIG. 1. Comparison of vertical dynamic pressure gradient from the non-hydrostatic model and the hydrostatic model with nonlinear approach. In each panel, the top figure is the non-hydrostatic model, the lower panel is the hydrostatic model. (a) wave amplitude / epilimnion depth (η_0/h_1) = 0.5 and grid of 0.5m x 0.5m, (b) (η_0/h_1) = 0.5 and grid of 0.25m x 0.25m, (c) (η_0/h_1) = 1.0 and grid of 0.5m x 0.5m, (d) (η_0/h_1) = 0.5 and grid of 0.25m x 0.25m. The colorbar represents the dynamic pressure gradient, as in eq. (3), units are m/s^2.

The nonlinear, hydrostatic model with a larger wave amplitude / epilimnion depth ratio (η_0/h_1) compares better with the non-hydrostatic model than the smaller η_0/h_1. Additionally, as the grid is refined, the nonlinear, hydrostatic model better captures the vertical dynamic pressure gradient, in terms of magnitude and spatial incidence. In all cases, the nonlinear, hydrostatic model under predicts the vertical dynamic pressure gradient from the non-hydrostatic model.

The hydrostatic, nonlinear model for the vertical dynamic pressure gradient yielded an adequate model which could then be applied to the non-hydrostatic factor. Eq. (3) was vertically integrated over a single cell and differentiated with respect to the horizontal direction, *x*, to yield a definition of the dynamic pressure gradient in the x-momentum equation with the known hydrostatic vertical velocity. This definition was then applied to the non-hydrostatic factor in eq. (1).

A two-dimensional domain (10m long and 7.5m water depth), with two different grid resolutions (0.5m x 0.5m and 0.25m x 0.25m), initialized with a non-hydrostatic internal wave of sinusoidal shape (epilimnion depth/ total depth = 0.5 and wave amplitude / epilimnion depth = 1.0) was used. This wave was chosen in accordance with the study of Horn, et al (2001) which classified internal wave behavior; the wave produces Kelvin-Helmholtz billow formations. To verify the ability of the non-hydrostatic factor to isolate where the dynamic pressure gradient is large, the non-hydrostatic factor was computed with the dynamic pressure derived from the hydrostatic velocity field using the nonlinear approach ("model non-hydrostatic factor") and compared to the non-hydrostatic factor computed with the actual dynamic pressure gradient from the non-hydrostatic model ("actual non-hydrostatic factor"). For both grid resolutions, the model non-hydrostatic factor basically matched the actual non-hydrostatic factor, as seen in fig. (2); however, it tended to under predict where the non-hydrostatic factor is large as did the nonlinear, hydrostatic model for the vertical dynamic pressure gradient. Additionally, in both cases when the billow formed and over-turned the non-hydrostatic factors had a very random pattern across the domain; this yields a non-hydrostatic factor that is only able to be used prior to billowing. The non-hydrostatic factor as it is currently evaluated, does not provide a complete picture of the domain with which regions where dynamic pressure affects the flow can be isolated.

CONCLUSIONS

The results presented above are preliminary, but show insight into how dynamic pressure is distributed through a domain. Although the results are currently inconclusive, they provide a platform from which the non-hydrostatic factor can be more completely examined and modified. This work, along with further investigation into the non-hydrostatic factor, will enable a domain to be separated into regions where dynamic pressure has an affect and where it does not, thus allowing the computational efficiency of the non-hydrostatic model to increase.

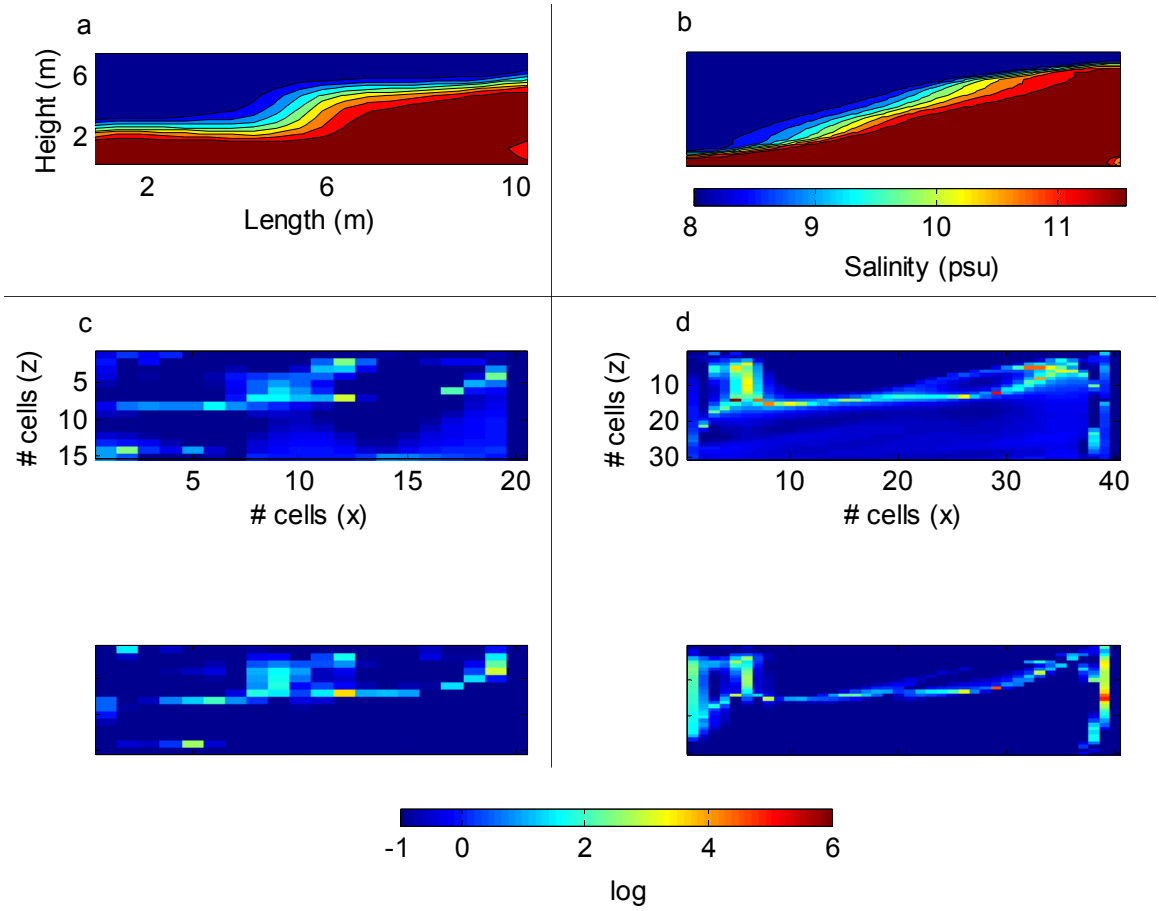

FIG. 2. Comparison of non-hydrostatic factor from non-hydrostatic model and hydrostatic model with nonlinear approach. (η_0/h_1) = 1.0, (a) and (c) gave a grid of 0.5m x 0.5m, (b) and (d) have a grid of 0.25m x 0.25m. (a) and (b) are the density profiles. In panels (c) and (d) the top figure is the actual non-hydrostatic factor and the bottom figure is the model non-hydrostatic factor. The colorbar for (c) and (d) represents the log of the non-hydrostatic factor.

ACKNOWLEDGMENTS

The authors would like to acknowledge: 1) support of the Office of Naval Research under grant N00014-01-0574, and 2) for the use and development of CWR-ELCOM.

REFERENCES

Hodges, B.R. (2000a), *Numerical Techniques in CWR-ELCOM*, Centre for Water Research, University of Western Australia, Technical Report WP 1422-BH.

Hodges, B.R. (2000b), "Evolution of Internal Waves in Hydrostatic Models," Office of Naval Research Young Investigator Program, Proposal.

Horn, D.A., J. Imberger and G.N. Ivey (2001), "The Degeneration of Large-scale Interfacial

Gravity Waves in Lakes," Journal of Fluid Mechanics, **434**, 181-207.
Kim, J. and P. Moin (1985), "Application of a Fractional-step Method to Incompressible Navier-Stokes Equations," Journal of Computational Physics, **59**, 308-323.
Stansby, P.K. and J.G. Zhou (1998), "Shallow-water Flow Solver with Non-hydrostatic Pressure: 2D Vertical Plane Problems," International Journal of Numerical Methods in Fluids, **28**, 541-563.

APPENDIX I. NOTATION

p_d dynamic pressure
u horizontal velocity
w vertical velocity
γ non-hydrostatic factor
ρ density
η_o wave amplitude
h_1 epilimnion depth